CLIMATE PATTERN RECOGNITION OVER 3000 YEARS OF THE HOLOCENE ONSET (8500 BC TO 5600 BC, PART 1 - UPDATED)

JOACHIM SEIFERT

FRANK LEMKE

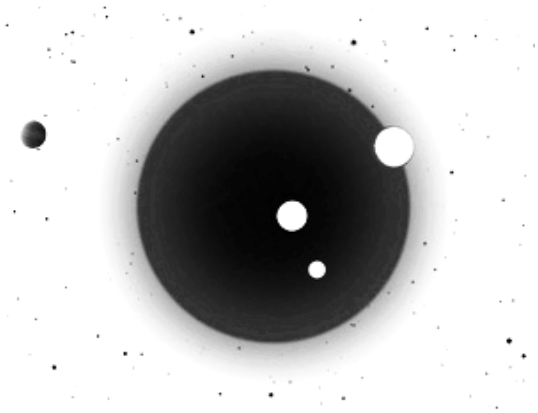

Correspondence to: weltklima@googlemail.com

Website: http://www.knowledgeminer.eu • http://www.climateprediction.eu

MARCH 2017

This is a revised version of the initial paper published in December 2014.

Abstract. Features and application of the Climate Pattern Recognition analysis for evaluating temperature evolution in Holocene time series are explained. We select as the first period, the early 3000 years of the Holocene. This study recognizes three distinct climate patterns, a multi-millennial pattern and two multi-centennial patterns. Special attention is given to peak temperature spikes. The analysis is able to distinguish drivers of climate change from Holocene temperature graphs, such as the celestial Milankovitch motion, Earth orbit oscillations and cosmic meteor impacts on Earth. We use the graphical version of GISP2 for visual demonstration of climate patterns. Each up and down of the GISP2 temperature curve is explained in detail by use of a new pattern recognition grid, which we place onto all time spans of the entire Holocene. A well-defined exact and continuous multi-centennial Holocene cycle with a successive growth of a 6.93 years has been identified, which, until present, had not been determined by other authors, because they only focus on constant, fixed-length cycles. This growing cycle with its exact timing over 10,000 years excludes an internal atmospheric-oceanic cycle cause and has no relation to multi-millennial Milankovitch cycles. We provide cycle beginning and end dates, exact to within a decade. The cyclic temperature amplitude can be determined by the quotient of 0.0037, with which each cycle period length can be converted into its proper cycle amplitude valid for the entire Holocene. The pattern recognition analysis demonstrates the celestial origin of three major climate forcing mechanisms and is superior to all GCM and other simulations. We will continue with the part 2 paper for the time span 7000 BC to 4700 BC. Eight successive papers will cover the entire Holocene.

Citations. Seifert, J., Lemke, F.: Climate Pattern Recognition over 3000 Years of the Holocene Onset (8500 BC to 5600 BC), 2017,
http://www.knowledgeminer.eu/climate_papers.html

1. INTRODUCTION

Holocene GCM climate models of type PMIP2/3 and CMIP3/5 underperformed in assessment of temperature evolution (McKitrick, 2014), global atmospheric circulation, precipitation in the Holocene (Alder and Hostetler, 2014), modeling the last interglacial (Bakker and Reussen, 2014), aeolian dust (Evan, 2014). Large Holocene periods remain in "conundrum" (Liu, 2014). For this reason, a different approach with high quality and reliability is required.

In this paper, we present our Holocene Climate Pattern Recognition Analysis, featuring a new pattern grid recognition method with which three major climate forcing mechanisms can clearly be identified and quantified. For performing our pattern recognition, we need a high resolution time series in graphical form, from which all patterns can be identified. The GISP2 ice-core temperature series (Alley, R.B. 2000) is an excellent reference, which we transformed into an equidistant time series with a resolution of 10 years to allow easy display of periodical causes. The resulting Holocene GISP2 graph and the time period discussed in this paper is shown in figure 1. For numerical values, we use (Alley, R.B. 2004).

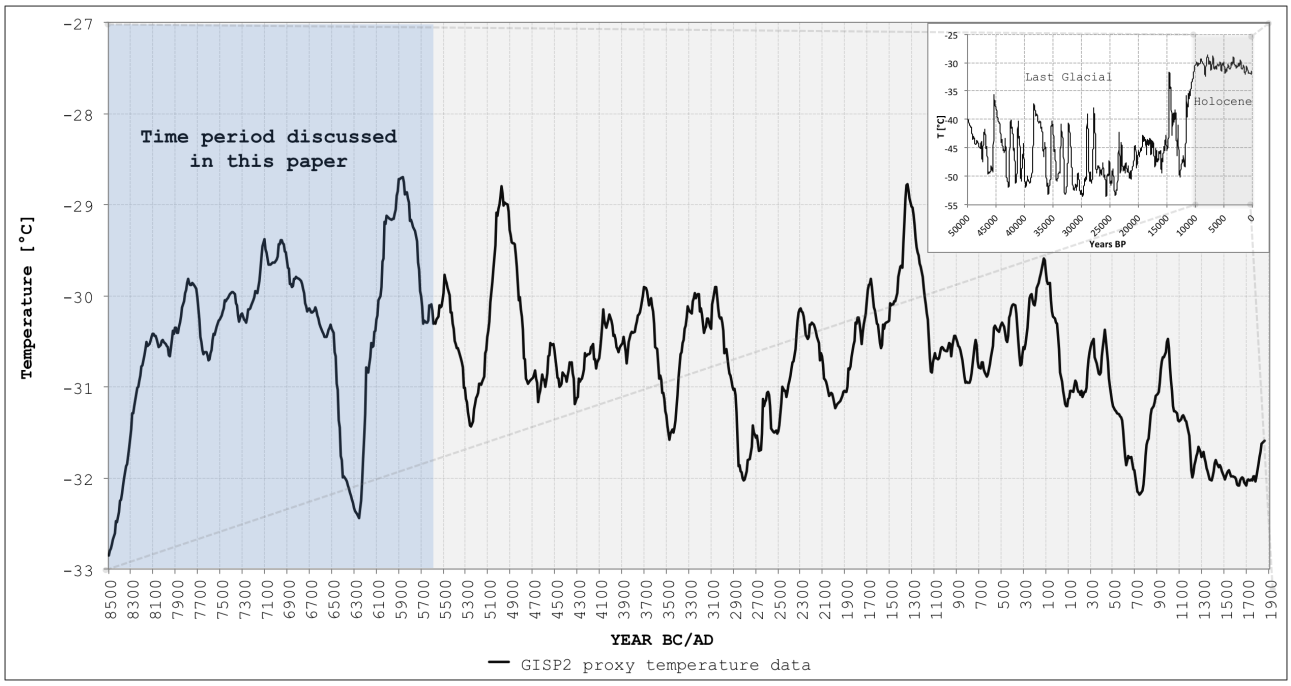

Figure 1. The Holocene GISP2 data and the period discussed in this paper (equidistant in time)

Our analysis is based on a pattern recognition grid, which consists of 3 major patterns.

2. THE LONG-TERM MULTI-MILLENNIAL PATTERN

The first component is the Milankovitch line, which represents a temperature line for the 100,000 year Sun motion cycle, which produces glacials and interglacials. The Sun motion is a slow motion following the path from one solar focus position towards the solar system center and continuing to the opposite side into the second focus position. This process has the duration of about 100,000 years; and interglacials are the result of the Sun´s stay in either focal position. By approaching a focal position, the Sun motion produces a steep temperature increase by coming out of the glacial and going into the new focal interglacial. The interglacial high temperature top is reached within the focal position center, descending slowly with the Sun´s return run back to the solar system center. This is standard feature of all previous interglacials. There is other literature, however, claiming Earth wiggling in a 41,000 year mode (obliquity cycle) produces interglacials, but this approach has not been substantiated for the evolution of past interglacials.

Let us look at the graph with the Milankovitch Sun motion line (fig. 2).

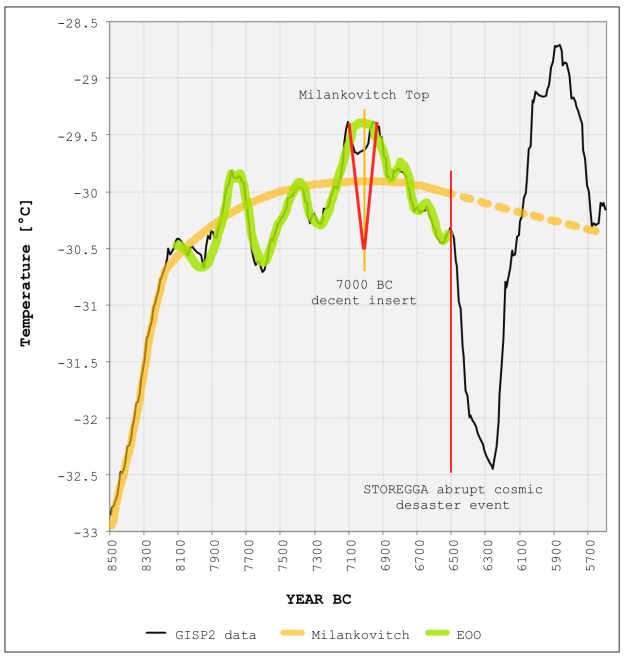

Figure 2. Milankovitch Line and GISP2

We can see the following: The millennial Milankovitch Sun motion line, from 8500 BC on, rises strong and unaltered by other climate forcing as a curvilinear line out of the glacial until 8150 BC. As this line reaches 8150 BC, a second and different, now centennial pattern develops: Temperatures start to oscillate around this Milankovitch line, which remains centered within those upcoming new oscillations. The Milankovitch line reaches its highest top in 7000 BC, the central solar focal point, at which the warmest millennial period of the entire Holocene is thus produced. From there on, the Sun´s motion toward the solar system center initiates and therefore, temperatures will decrease. A triangular descent insert indicates the Sun´s directional change, which also explains this temperature feature: "peak (7100 BC) to trough (7000 BC) to second peak (6950 BC)". This triangular insert will repeat once again, at a later date, within the Roman Warm Period, as described in detail in part 6 of this Holocene series.

After the 7000 BC Holocene top, the Milankovitch line descends at a pace of 0.40 C per millennium, which can be measured by prolonging the descending trend line.

3. THE REGULAR MULTI-CENTENNIAL PATTERN OF THE EARTH ORBIT OSCILLATION

At first, a few introductory remarks on multi-centennial cycles:

There are so-called Bond-cycles and Dansgaard-Oeschger cycles, but their proper cycle beginnings and endings are never listed. Another cycle paper (Evangelista, 2014) employs the Morlet-wavelet analysis for the time period 11,100 BC to 2,100 BC, and detects "marked periodic signals of ~0.8, ~1.7 and ~2.2 kyrs". Another author, Soon, W (Soon 2014) identified "intermediary derived cycles of 700 and 300 years".

The deficiency in those studies is their limited search for fixed, constant only cycles, instead of dedicating attention to astronomically growing cycles or stochastic cyclic patterns. The present multi-centennial growing cycle has been calculated in theory by (Seifert, J. 2010), awaiting empirical confirmation by the present Holocene study; additional literature is (Seifert and Lemke, 2012).

Demonstrating a well-defined periodicity would prove an indisputable external celestial cyclic forcing, because, as Stocker showed in 1992 (Stocker and Mysak, 1992), that the internal atmosphere-ocean climate system is unable to produce a forcing with "a single, well defined periodicity". The existence of a growing cycle would permit us to substitute major internal climate forcing by a periodic cosmic Holocene climate drivers (fig. 3).

We see the following: The yellow Milankovitch line helps us to identify the central line between oscillations either to the above or to below the line. Before analyzing temperature oscillation amplitudes, we identify the regular oscillation period in 3 steps:

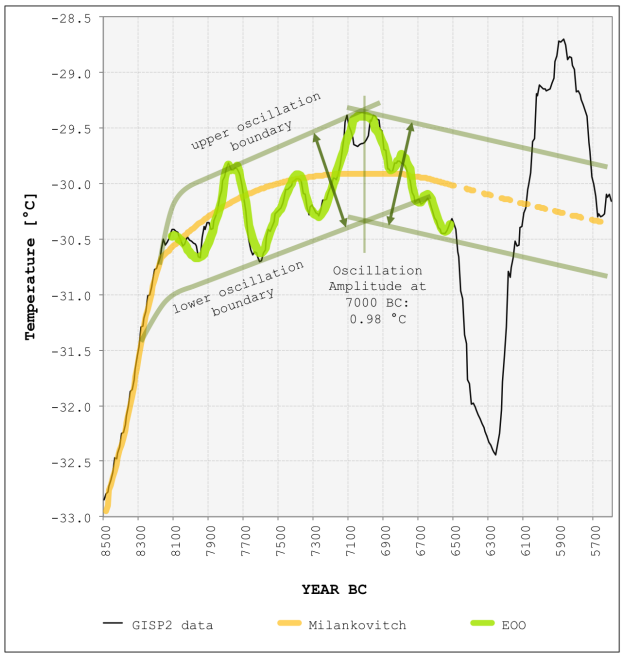

Figure 3. Formation of EOO Wave

At first, in order to determine cycle amplitudes, we connect peak points of waves and half-waves in the graphic picture. Those connections represent one upper cycle boundary line and one lower cycle boundary line. At the point 7000 BC, both lines are by an amplitude of 0.98ºC (GISP2 borehole degrees) apart. We may take this value and divide it by the quotient of 0.0037, and we obtain the resulting cycle period length (in this case: 266 years). The literature (Seifert, 2010) proves the linear relationship between cycle amplitude and cycle period. Unfortunately, after the date of 6510 AD, the visible cycle amplitude remains overpowered by a cosmic meteor strike, but continues unabated masked in the background. The same relates to the millennial Milankovitch line: The line maintains its central path between the upper and the lower oscillation cycle line.

As next, we determine the cycle period length with the following method:

Step 1: We take the first oscillation high peak, BC 8108, as center of a plateau BC 8144-8102. As next peak event 1,000 years later, we take BC 7114. Between those two dates we observe 4 half-wave periods, which are supposed to be growing: At 7000 BC, the period was calculated to be 266 years already, and we now set the initial cycle length to 238 years and all following cycles to grow by 7 years.

Step 2: We set the half-wave oscillation period of 238 years, its starting point at 8108 BC as initial cycle period and prolong it by 7 years for each following period. We arrive at the time series (minus sign stands for BC): BC 8108 (238 yrs), -7870 (245 yrs), -7625 (252 yrs), -7373 (259 years), -7114 (266 years), -6848 (273 years), -6576 (280 years), -6296 (286 years), -6010 (293 years), -5716 (300 years) and continue this growing cycle for the following 10,000 years. Additionally, we compared this 7 year periodicity growth to the cycle outcome in the late Holocene and decided to shorten this 7 year growth by a percentage of 1%, thus a slightly shorter 6.93 year cycle period growth. This shorter value matches late Holocene temperature peak dates better.

We provide the first 10 cyclic oscillation period peaks; dates and temperatures were taken from Alley (Alley, 2004).

1. Peak event BC 8108:
   Temps rising: -8149 = -30.55° … -8126 = -30.48°,
   T. high temp plateau -8114 = -30.41° to -8102 = -30.41° Temps falling from -8102 = -30.41° to low at 8078 = -30.43°
   = Peak event exact on plateau
2. Peak event BC 7870:
   Temps rising: -7929 = -30.46° to -7907 = -30.33° T. short low peak at -7884 = -30.42°
   Temps rising: -7860 = -30.31° to -7834 = -30.10°
   = Peak event difference 14 years
3. Peak event BC 7625:
   Temps falling: -7651 = -30.61° to -7629 = -30.62°
   T. low peak at -7606 = -30.71°
   Temps rising -7582 = -30.60° …. -7560 = -30.46°
   = Peak event difference 19 years
4. Peak event BC 7373:
   Temps rising: -7436 = -30.03° to -7416 = -29.98°
   T. high plateau -7395 = -29.95° to -7373 = -29.97
   Temps falling -7352 = -30.09°
   = Peak event on plateau
5. Peak event BC 7114:
   Temps rising: -7151 = -29.84° to -7132 = -29.59°
   T. high peak -7111 = -29.44°
   Temps falling -7091 = -29.52° to -7071 = -29.65°
   = Peak event difference 3 years
6. Peak event BC 6848:
   Temps falling -6892 = -29.69° to -6872 = -29.86°
   T. low peak -6853 = -29.89°
   Temps rising -6835 = -29.82° to -6816 = -29.79°
   = Peak event difference 5 years
7. Peak event BC 6576:
   Temps falling -6608 = -30.30° to -6588 = -30.39°
   T. low peak -6569 = -30.45°
   Temps rising -6549 = -30.45° to -6530 = -30.38°
   = Peak event difference 7 years
8. Peak event BC 6296:
   Temps falling -6300 = -32.31° to -6280 = -32.40°
   T. low peak -6260 = -32.44°
   Temps rising -6240 = -32.23° to -6221 = -31.80°
   = Peak event difference 36 years

9. Peak event BC 6010:
   Temps rising -6043 = -29.64° to -6024 = -29.23°
   T. high peak -6007 = -29.13°
   Temps falling -5989 = 29.14° to -5971 = -29.16°
   = Peak event difference 3 years
10. Peak event BC 5716:
   Temps falling -5728 = -29.59° to -5692 = -30.09°
   T. low peak -5659 = -30.29°
   Temps rising -5642 = -30.28° to -5624 = -30.12°
   = Peak event difference 57 years.

General peak event differences arise out of GISP2 sample timing, which was not done taking wave periodicities into account. The two outlying dates of periodicities no. 8 and no. 10 can be explained by the power of the Storegga cosmic impact (explained in the following section), which prolonged those two cold spike events by 36 and 57 years. We demonstrate cycle periods in figure 4.

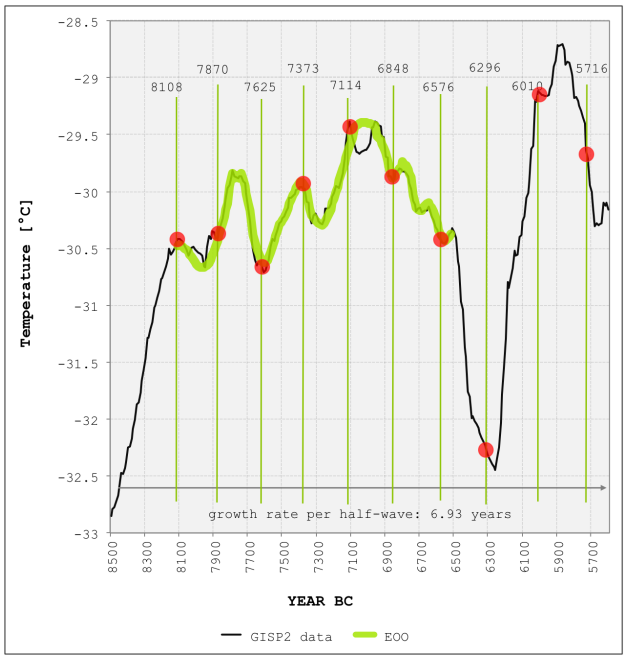

Figure 4. EOO cycle dates

Cycle period dates are presented as vertical lines, in order to produce a grid pattern made out of vertical and horizontally inclined lines.

A final remark to the origin of the EOO Earth orbital oscillation pattern. It is not a Milankovitch cycle pattern, because Milankovitch left orbital oscillations entirely out of consideration. The cycle is the entirely different Earth "osculation" cycle, as described by the mathematicians Isaac Newton and Carl Gauss (Gauss, 1809).

After placing the cycle grid onto the temperature graph, we can detect the following feature.

4. THE ABRUPT, STOCHASTIC, Z-SHAPED MULTI-CENTENNIAL PATTERN

As shown in figure 5, we can observe that from the periodicity peak at 6576 BC, temperatures rose upwards to form the next, following half-wave period. But, after a rise of 70 years, at 6510 BC, a powerful interruption of the oscillation pattern occurred, the so-called "8.2 kiloyear event". This event marks our third recognizable pattern: A multi-centennial, interrupting, Z-shaped, double-spike pattern. It consists of a large cold spike, always occurring at first, followed by a large hot spike. This strong double-spike pattern overrides, cancels out and masks the visible periodicity of the half-wave cycle line. But the cyclic EOO orbital oscillation pattern continues unabated invisibly in the background and will resurface again, once overriding cosmic impact forcing abated.

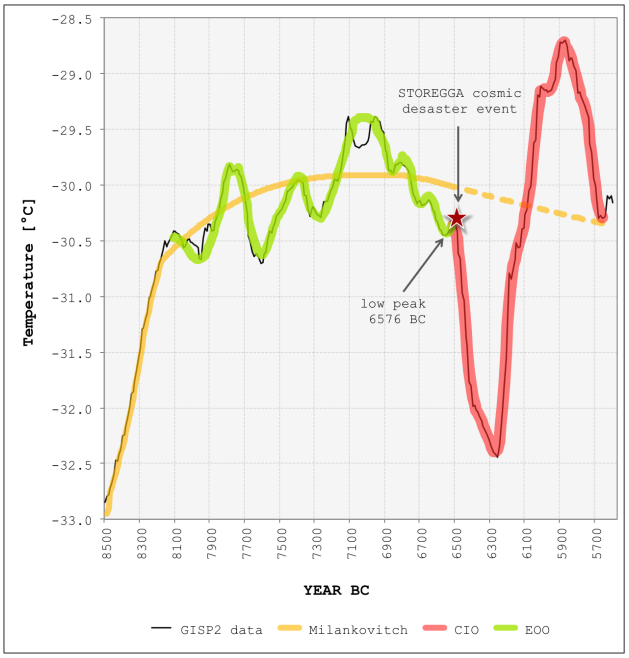

Figure 5. The cosmic impact oscillation pattern (CIO)

The two patterns, the regular cyclic orbital oscillation pattern, together with the strong stochastic disturbance pattern, shape the temperature evolution of the entire Holocene to a large extent.

The major feature of the double-spike pattern are pronounced cold and hot temperature spikes, in comparison to rather round shaped half-wave periodicity peaks. The double-spike temperature oscillation is the typical feature of all cosmic meteor impacts on Earth, i.e., there cannot be a sizable cosmic meteor impact (crater diameter larger than 100 m) on Earth without a presence of this major impact feature in GISP2. The mechanics of this process is explained in (Seifert and Lemke, 2012).

Additionally, this temperature swing must correlate to impact craters sizes, i.e., small meteor impacts produce

small Z-shaped temperature swings, and large impacts produce large temperature swings in GISP2.

The cosmic meteor impact at 6510 BC is known as "Storegga slide". The meteor bolide hit the headwall of the Norwegian continental shelf, coming in from the East, flying to the West, producing a crater located 200 m below ocean level, which in turn pushed and littered an enormous rock volume from the steep continental edge over hundreds of kilometers into flight direction along the ocean floor. Most Storegga literature, at present, hypothesize the slide as being an earthquake slide and doubt it at the same time , because this enormously huge slide volume is too high for an earthquake effect. The displaced rock mass is estimated at an 2,500-3,200 km3 volume. As comparison, two large historical volcano mega-eruptions, ejected 10 km3 mass volume (Pinatubo eruption, AD 1991) or 60 km3 mass volume (the giant Thera-Santorini eruption, 1603 BC). Methane pressures in sediments were hypothesized as additional triggering force, but there is not enough so-called "suspected gas hydrate pressure", because the whole area is covered by multitudes of "pockmarks". Those pockmarks are large vertical gas pressure relief vents, continuously discharging underground methane, continuously relieving gas pressures, therefore, there cannot be an excessive gas pressure build-up. The Storegga slide is a cosmic meteor impact. The impact crater lies at the coordinates of 64°N and 5°E. The crater is well visible on perspective seafloor bathymetric maps. Comprehensive evidence will be given in a separate Storegga cosmic impact paper. Seafloor mapping identified a total of four craters (Solheim and Bryn, 2005). The complete Storegga double-spike meteor impact pattern lasts from 6510 BC to 5700 BC.

One observation concerning other climate Storegga ("8.2 kyr event" or "Bond event") literature: This impact event is a frequent topic in Holocene papers which are always based on computer simulations. All those simulation papers exhibit one common feature: They elaborate only the cold spike of the Z-shaped pattern and always exclude the following hot spike. The reason for this is that cold spikes can conveniently modeled by an assortment of alleged climate "cold drivers," such as Laurentide ice mass losses, ice rafting, ocean flow, low sunspots etc… but all of those are unsuitable to explain the second double-spike pattern part, the ensuing hot spike. Therefore, all simulation papers carefully do not mention the hot spike.

One last remark concerning volcano mega-eruptions: The assumption is that multi-decadal temperature dips should occur after VEI 6, 7 and 8 mega-eruptions of volcanos, which cause stratospheric dimming for decades, and temporary cooling. Calculations for regular eruption effects are made in (Wahl, 2014), showing "a clear and robust 3 - 5 years La Nina-like response".

The best study is those of Sigl, M. (Sigl and Winstrup 2015), which demonstrates that in the past 2,500 years, all volcano effects on global temperatures had a maximum duration of 10 years only. Therefore, those short volcanic eruption effects of less than 10 years remain invisible in GISP2.

5. SYNOPSIS

We combine all climate forcing patterns into one single graphic, shown in figure 6.

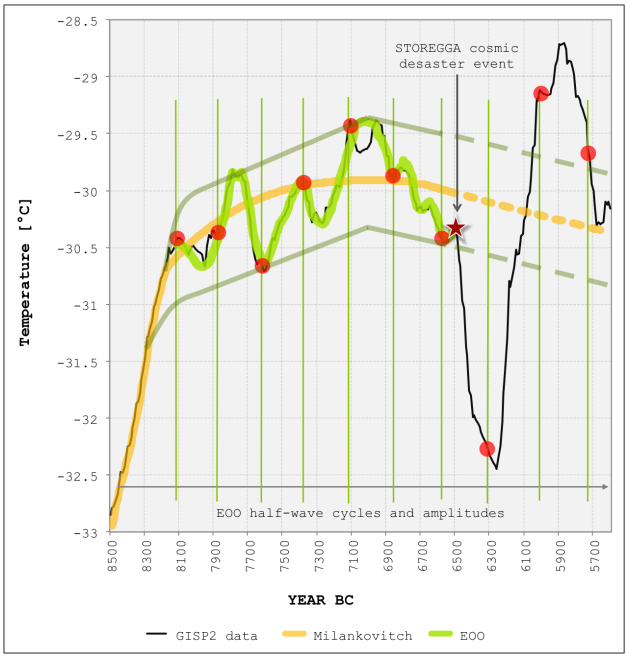

Figure 6. Temperature pattern synopsis

The pattern recognition analysis places its pattern recognition grid of vertical and horizontal lines onto all sections of the Holocene. This method achieved the identification of three cosmic climate forcing mechanisms: The Milankovitch Sun motion cycle, the growing EOO multi-centennial cycle and the double-spike cosmic meteor impact pattern. We show that the 100,000 year Milankovitch cycle line rises steep out of the last glacial. Then, by 8100 BC, gradually and still irregular, Earth orbit oscillations emerge, deviating global temperatures. This is dictated by a celestial mechanism, which produces a well-defined multi-centennial oscillation pace which prolongs by 6.93 years for each successive cycle period. All cycle dates are provided. Cyclic periods and amplitudes are in linear relation with the factor 0.0037, which we apply to convert each period length into its individual cycle amplitude. This factor is valid for the entire Holocene. At 7000 BC, the peak of the regular Holocene is reached, from

where on, out of a triangular decline insert, the rising Milankovitch temperature line now turns downwards. After a 500 year temperature decline, the cyclic temperature evolution suddenly becomes masked, starting 6510 BC, when a large cosmic meteor hit Earth, initiating an enormous, double-spike temperature oscillation swing: At first,a strong cold spike, the "8.2 kyr event", followed by the hot spike. This oscillation swing, a standard feature for all and every cosmic meteor impacts on Earth, ends in 5600 BC, when temperatures finally have regressed to close to their initial 6510 BC level.

REFERENCES AND SOURCES

Alder, J.R.; Hostetler, S.W.: Global climate simulations at 3000 year intervals for the last 21000 years with the GENMOM coupled atmosphere-ocean model, Clim. Past. Discuss., 10, 2925-2978, 2014, DOI: 10.5194/cpd-10-2925-2014

Alley, R.B.: The Younger Dryas cold interval as viewed from central Greenland, Quaternary Science Reviews, Volume 19, Issues 1-5, 2000, http://www.ncdc.noaa.gov/paleo/icecore/greenland/greenland.html,

Alley, R.B., 2004. GISP2 Ice Core Temperature and Accumulation Data.IGBP PAGES/World Data Center for Paleoclimatology, Data Contribution Series #2004-013, NOAA/NGDC Paleoclimatology Program, Boulder, CO, USA

Bakker, P.; Reussen, H.: Last interglacial model-data mismatch of the thermal maximum temperatures partially explained, Clim.Past.,10, 1633-1644, 2014, DOI: 10.5194/cp-10-1633-2014

Evan, A.T., et.al.: An analysis of aeolian dust in climate models, Geophys. Res. Lett., 41, online 18.Aug. 2014, DOI: 10.1002/2014GL060545

Evangelista, H.; et.al.: South Tropical Atlantic anti-phase response to Holocene Bond Events, Palaeogeography, Palaeoclimatology, Palaeooecology, vol. 415, Dec. 2014, p. 21-27, doi: 10.1016/j.palaeo.2014.07.019

Gauss, Carl: Theoria Motus Corporum Coelestium, Perthes&Besser publishers, Hamburg, 1809, http://dx.doi.org/10.3931/e-rara-522

Liu, Z. et. al.: The Holocene Temperature Conundrum, PNAS, vol. 111, no. 34 (2014) DOI: 10.1073/pnas.1407229111

Mauget, S.A.; Cordero, E.C.: Optimal Ranking Regime Analysis of Intra- to Multi-Decadal U.S. Climate Variability, AMS, Journal of Climate, e-view, 2014, DOI: http://dx.doi.org/10.1175/JCLI-D-14-00040.1

McKitrick, R.R.: HAC-robust Measurement of the Duration of a Trendless Subsample in a Global Climate Time Series. Open Journal of Statistics, 4, 2014, pp527-535, http://dx.doi.org/10.4236/ojs.2014.47050

Pielke, Sr., R.A.: Mesoscale meteorological modelling, 3rd. edition, Academic Press, 2013, 760 p., ISBN 9780123852373, chapter 7 and 8

Seifert, J.: Das Ende der globalen Erwärmung, Berechnung des Klimawandels, ISBN 978-3-86805-604-4, Pro Business Verlag, 2010, 109 pages, pp.53-56 www.book-on-demand.de

Seifert, J., Lemke, F.: Five climate forcing mechanisms govern 20,000 years of climate change, 2012, http://www.knowledgeminer.eu/climate_papers.html

Sigl, M.; Winstrup, M., et. al.: Timing and climate forcing of volcanic eruptions for the past 2,500 years, Nature 523, 543-549 (30 July 2015), doi: 10.1038/nature 14565

Solheim, A., Bryn, P: Ormen Lange - An integrated study for the safe field development in the Storegga slide area, Elsevier, 2005, ISBN 0080446949, p.1-10, reprint from Marine and Petroleum Geology, vol. 22/1-2, 2005

Soon, W.; et.al.: A review of Holocene solar-linked climatic variation on centennial to millennial time scales: Physical processes, interpretative frameworks and a new multiple cross-wavelet transform algorithm, Earth-Science Reviews, vol. 134, Jul 2014, p.1-15, doi: 10.1016/j.earscirev.2014.03.003

Stocker, T.F., Mysak, L.A.: Climatic fluctuations of the century time scale: A review of high-resolution proxy data and possible mechanisms, Climate Change, 20, p. 227-250, March 1992, Kluver Academic Publishers, N.L., http://www.climate.unibe.ch/~stocker/papers/stocker92cc.pdf

Wahl, E.R., et.al: Late winter temperature response to large tropical eruptions in temperate western Northern America: relationship to ENSO phases, Global and Planetary Change, vol. 122, 2014, pp. 238 - 250, DOI: 10.1016/j.gloplache.2014.08.005